

PROJECTILE EFFECTS ON CRATER DIAMETER AND DEPTH SCALING IN METAL TARGETS. P.H. Schultz¹ and R. T. Daly². ¹Department of Earth, Environmental and Planetary Sciences, Brown University, 324 Brook St., Box 1846, Providence, RI, 02912 (peter_schultz@brown.edu). ²The Johns Hopkins University Applied Physics Laboratory, 11101 Johns Hopkins Road, Laurel, MD, 20723, USA.

Introduction: Many experiments have examined the effect of impact speed [e.g., 1-4] and angle [4-5] in various metals on cratering efficiency and crater shape. Here we explore the effects of different impactor types on metal targets and assess the processes affecting scaling, beyond the role of target strength.

Background: Laboratory [4,5] and computational [6] experiments suggest that energy controls cratering efficiency in strength-controlled targets. Energy-controlled scaling results predicts [5] that cratering efficiency (displaced target mass, M , scaled to projectile mass, m) should depend on the cube root of the vertical component [6] of impact velocity (v), i.e., $M/m \sim (v^2 \sin^2 \theta)^\beta / Y$, where θ = the impact angle (from the horizontal), β is a scaling exponent that ranges from 1/3 (energy) to 1/2 (momentum), and Y is a measure of strength. Other studies, however, indicate that oblique impacts can result in significant fractions of the energy retained by the surviving (decapitated) projectile fragments [8,9]. If conditions generated at first contact controls the peak pressure, then energy carried away by the projectile (and projectile fragmentation) might not be expressed in crater-scaling relations. The following experiments were designed to determine if this assumption is correct in four ways: different projectile types for a given target; different target types for a given projectile; isolating the effects of first contact by using cylindrical targets; and use of a low-impedance surface layer. The experiments were performed at the NASA Ames Vertical Gun Range in support of a study to assess the effects of projectile fragmentation and survival.

Results: Rather than cratering efficiency, the study here examines just the maximum transverse diameter (D) and maximum crater depth (p) for different target and projectile types. In order to assess the effect of first contact, projectiles included copper, steel, aluminum, serpentine, quartz, and Polyethylene with impact angles from 15° to 90° (from the horizontal). Targets included aluminum, steel, and iron meteorites (Gibeon). Figure 1a first illustrates the effect of different projectile types for impacts into aluminum targets with the following scaling dependence: $(X/a)(\delta_t/\delta_p)^{1/3} \sim (\delta_t v^2 \sin^2 \theta)^\beta$ where X represents either diameter or depth. Scaling with $\beta \sim 1/3$ applies for diameter > 30° but not for depth: lower projectile density results in much smaller scaled depths with much larger values of β .

Fig. 1a also includes the scaled diameters resulting from serpentine and quartz projectiles into steel and meteorites. Data from impacts into steel or meteorite

targets should be offset from data for aluminum targets because differences in strength have not been included. The contrast between the serpentine and spherical quartz projectiles, however, is curious. Figure 1b introduces a factor of 4 in order to bring the steel and meteorite targets in line with the aluminum targets. Such a correction, however, is much larger than the known steel-to-aluminum strength ratio. Quartz projectile data, however, remain offset below expectations.

Figure 2a considers a different scaling relation for crater depth: $(p/a)(\delta_t/\delta_p)^{1/3} \sim (\delta_p v^2 \sin^2 \theta)^\beta$ where the dependence incorporates projectile, rather than target, density. This assumption not only accommodates the different density projectiles for the aluminum but also accommodates the impacts into steel (and meteorites), even without accounting for differences in target strength. For impact angles below 45°, the value of the scaling exponent (β) approaches 0.75, which is inconsistent with either energy or momentum scaling.

The effect of surface curvature and a low-impedance surface layer [10] is shown in Figure 2b. In this case, a single target type is used (aluminum). This strategy removes the contribution from the failed projectile (downrange scouring). Crater depth now decreases with a decreasing ratio of cylinder radius (R) relative to the projectile radius (r) as a result of projectile decoupling during first contact.

Discussion: The results can be explained by two different processes. First, two different strength terms must apply to the crater diameter and depth. Crater diameter depends on tensile (or shear strength), whereas the depth depends on the yield strength, which is nearly the same for steel/meteorites and aluminum. Figure 1 reveals, however, that this correction does not accommodate the contrast in transverse crater diameters for quartz projectiles and serpentine projectiles. Second, target strength effects must be only part of the answer (Fig. 2). At low impact angles (< 45°), the projectile fragments and decouples at first contact and continues downrange to form a scoured ledge or sibling craters [8]. As a result, the projectile interacts (and removes) target material downrange, after the initial conditions that control the transverse diameter. Placing a thin (1/4 projectile diameter) low-impedance target on top an aluminum target (not shown) results in plastic deformation in the aluminum with a depth consistent with expectations (including the thickness of the layer). The effect of the failed projectile (gouging and re-impacts) is missing.

While the transverse crater diameter scales with an exponent $\beta \sim 1/3$ (except at angles below 30°), the depth scales with a much larger exponent $\beta \sim 0.75$ due to decoupling of the projectile. This is reflected in the displaced mass ratio exponent $\beta (= 1.01)$ for oblique impact data (including $\sin \theta$), which is higher than that ($\beta = 0.79$) for vertical impacts predicted from computational models [6]. Consequently, crater scaling relations for oblique impacts into strength-controlled targets is affected by more than just initial coupling. Results reveal three overlapping processes: first-contact shock (controlling transverse diameter), plastic deformation (controlling depth), and shear/gouging/impacts from decapitated impactor fragments (affecting cratering efficiency and morphology). Projectile failure is controlled by impact angle, strength, and impedance contrast with the target [e.g.,8]. Hence, an impedance ratio should be included in complete scaling relations for strength-controlled targets.

Implications: Missions to high-density, strength-controlled asteroids (e.g., Psyche) may reveal very different crater morphologies and depth-to-diameter ratios at the same diameter. Moreover, crater ages based on the statistics of their diameters, however, may not be straightforward. Rather, crater depth (and perhaps displaced mass, see [11]) may be a more relevant metric for half the crater population (those formed at $<45^\circ$).

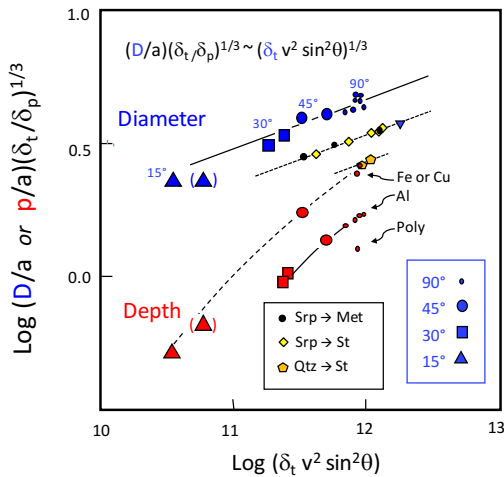


Fig. 1a: Relation between scaled transverse diameter, D , and depth, p , and assumed independent variables (including the target and projectile density ratio but excluding strength) for oblique impacts into aluminum (blue and red symbols). In addition, the effects of different types of projectiles into aluminum (labeled) as well as serpentinite and quartz into meteorite (black) and steel targets are shown. The diameter for a given target follows expectations, but depth does not. Instead, depths fall along parallel lines, offset according to projectile density.

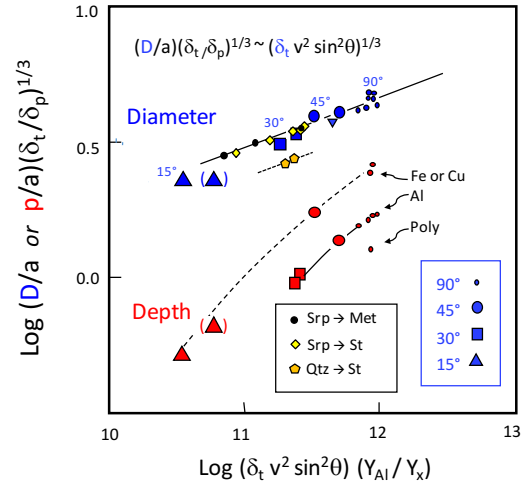


Fig. 1b: This is the same plot as in Fig. 1 but introduces a factor of 4 between the tensile (shear) strength in aluminum (Y_{Al}) and steel and meteorite (Y_X) targets to crater diameter, a factor greater than cited values for the different target strengths. Data for impacts by quartz spheres into steel targets, however, remain offset.

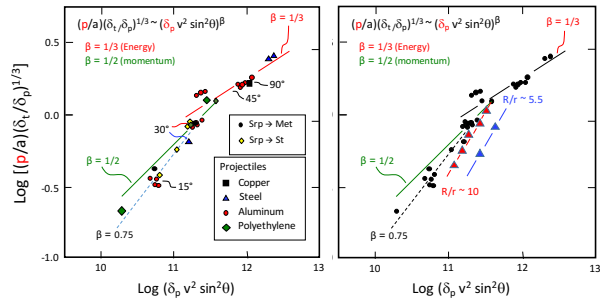


Fig. 2a: Crater depths for impacts by different projectiles (labeled) at different angles into aluminum, meteorites (yellow diamonds), and steel (black dots) without introducing any correction for contrasting target strength. **Fig. 2b:** Same as Fig. 2a but including the effect of surface curvature from impacts into aluminum cylinders for different relative sizes. As the radius of the impactor (r) becomes larger relative to that of the cylinder, the crater depth decreases (see text).

References: [1] Denardo, B. P. *et al.* (1967), NASA TN D-4067; [2] Christiansen *et al.*, 1993, *Int. J. Impact Eng.* 14, 157-168; [3] Bernhard and Horz, 1995, *Int. J. Impact Eng.* 17, 69-80; [4] Burchell and Mackay, 1998, *J. Geophys. Res.* 103, 22761-22774; [5] Holsapple, K. A., 1987, *Int. J. Impact Eng.* 5, 343-355; [6] Davison *et al.*, 2011, *MAPS*, 46, 1510-1524; [7] Gault and Wedekind, 1978, *Proc. 9th LPSC*, 374-376. [8] Schultz, P. H. and Gault, D. E., 1990, *GSA Sp. Paper 247*, 239-261; [9] Schultz and Crawford, 2011, *GSA Sp. Paper 477*, 141-159; [10] Schultz and Crawford, 2016, *Nature*, 535, 391-394; [11] Light *et al.*, 2018, *LPSC 50* (this volume).